BUNDLE ADJUSTMENT OF MARS HIRISE ORBITER STEREO IMAGES BASED ON THE RIGOROUS SENSOR MODEL

Yunhang Chen
Mapping and GIS Laboratory, Dept. of Civil and Env. Eng. & Geodetic Science
The Ohio State University
470 Hitchcock Hall, 2070 Neil Avenue, Columbus, OH 43210-1275
chen.1256@osu.edu

KEY WORDS: Digital Photogrammetry, Sensor Models, Adjustment, Topographic Mapping, High Resolution Image, Extraterrestrial

ABSTRACT:

Launched in August 2005, the Mars Reconnaissance Orbiter (MRO)'s primary goal is to obtain detailed morphologic information on the Martian surface using its onboard HiRISE sensor with a 0.3-meter ground resolution. However, inconsistencies between HiRISE stereo images must be removed based on the rigorous sensor model for the best level of accuracy. The new rigorous sensor model is developed specially for HiRISE due to its unusual complex camera design so that the mosaic of multiple image strips could be processed simultaneously under a uniform sensor model. A bundle adjustment (BA) based on this rigorous sensor model is implemented on two stereo pairs covering Husband Hill and Victoria Crater. After BA, the significantly reduced back projection residuals indicate that the inconsistencies are removed and the refined exterior orientation parameters are ready for mapping the Martian surface. Furthermore, 4 ground points measured from geo-registered Spirit rover images are incorporated into the BA as ground control points. Reduced inconsistencies on ground features between orbital intersection and measurements from rover images after BA indicate the mapping potential of orbital-ground integration. Small motions of the spacecraft around its nominal pointing, called jitter, has been detected on HiRISE trajectory data. The topographic effect of jitter is evaluated in this paper. Though its effect is insignificant when mapping small areas, further investigation needs to be performed so that the effect can be removed or reduced when mapping large areas.

1. INTRODUCTION

The Mars Reconnaissance Orbiter (MRO) has collected mapping data at an unprecedented level of accuracy on the Martian surface. Its primary scientific objectives are to characterize the surface, subsurface and atmosphere of Mars and to identify potential landing sites for future missions (NASA/JPL). HiRISE, the linear pushbroom image sensor onboard MRO, provides images with up to 0.3-meter resolution. This ultra-high resolution makes great progress possible in the derivation of topographic information on the Martian surface.

In order to support the Opportunity rover operation in the 2003 Mars Exploration Rover (MER) mission, a DEM of Victoria Crater was generated by USGS using HiRISE stereo images. A program was used to transform input raw images by projecting them into ground coordinates and then back into the image coordinates of an idealized HiRISE camera that can be modeled in the commercially available photogrammetry system SOCET SET. Photogrammetric processing of the transformed images is conducted using SOCET SET; the DEM is then generated based on the output results (Kirk, et al., 2007). However, in order to reach the best achievable mapping accuracy, inconsistencies between HiRISE stereo pairs must be removed based on the rigorous sensor model. Subsequently, this paper proposes a bundle adjustment to remove such inconsistencies using the rigorous HiRISE sensor model. Instead of using the commercial photogrammetric software used in the method described above, we are using our own code to incorporate the rigorous sensor model. Therefore, our results are free of errors caused by topography variation and can achieve the best level of accuracy can be reached.

2. RIGOROUS HiRISE SENSOR MODEL

2.1 Interior Orientation Modeling

The HiRISE camera is characterized by high signal-to-noise ratio (SNR) and large image size in addition to high resolution. Fourteen CCD arrays are distributed on its focal plane (Figure1). Each CCD array contains a 2048-pixel-wide line detector to build up an image in pushbroom mode, but with up to 128 lines of time delay and integration (TDI) to ensure a high SNR even in some extreme conditions. Ten of the 14 of the detectors, designed to accept only the red wavelengths, are overlapped one by one on the focal plane in the cross-track direction to provide continuous coverage of a 20,000-pixel-wide swath. The images provided by the red detectors mainly serve the purpose of morphologic studies. The other four detectors are sensitive to the blue-green and near-infrared (NIR) wavelengths. They allow for false-color imaging of the central 4000 pixels of the swath. The length of the along-track images that can be acquired depends on the number of CCDs used, pixel binning and data compression (Kirk, et al., 2007).

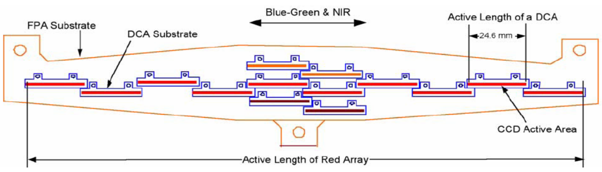

Figure1. HiRISE CCD structure on its focal plane (A. McEwen, et al., 2007)

HiRISE interior orientations, describing the geometry inside the camera, are provided in the USGS ISIS 3 HiRISE Instrument Kernel. The physical position of a pixel with respect to the perspective center can be calculated using its row and column indices in three steps. First, the pixel position with respect to CCD center is calculated using the formulas below.

$$\begin{aligned} ROW &= \mathrm{TDI}/2 - 64 - (\mathrm{BIN}/2 - 0.5) \\ COLUMN &= (\mathrm{m} - 0.5) \times \mathrm{BIN} - 1024 \end{aligned} \quad (1)$$

ROW and COLUMN are the indices with respect to CCD center; TDI and BIN are TDI and binning mode from the image header; "m" means the column index from image point measurement. Then, this row and column indices are converted to physical position with respect to the perspective center with Equation 2.

$$\begin{aligned} \mathrm{x} &= \mathrm{tx}_{i,0} + \mathrm{tx}_{i,1} \times COLUMN + \mathrm{tx}_{i,2} \times ROW \\ \mathrm{y} &= \mathrm{ty}_{i,0} + \mathrm{ty}_{i,1} \times COLUMN + \mathrm{ty}_{i,2} \times ROW \\ z &= -f \end{aligned} \quad (2)$$

Where x, y and z are the physical coordinate of the pixel center with respect to the perspective center. $\mathrm{tx}_{i,0} \cdots \mathrm{ty}_{i,2}$ are calibration parameters of the i^{th} CCD array. f is the focal length of HiRISE which is calibrated as 11994.9988mm. The calibration data of the sensor is provided by R.L. Kirk from USGS. Finally a radial distortion needs correction for the best level of accuracy. The radial distortion is modeled as:

$$\begin{aligned} \mathrm{r}^2 &= \mathrm{x}^2 + \mathrm{y}^2 \\ \mathrm{x}_p &= \mathrm{x} - (\mathrm{k}_0 + \mathrm{r}^2\mathrm{k}_1 + \mathrm{r}^4\mathrm{k}_2)\mathrm{x} \\ \mathrm{y}_p &= \mathrm{y} - (\mathrm{k}_0 + \mathrm{r}^2\mathrm{k}_1 + \mathrm{r}^4\mathrm{k}_2)\mathrm{y} \end{aligned} \quad (3)$$

k_0, k_1 and k_2 are distortion parameters; x, y are the coordinates from the previous step; $\mathrm{x}_p, \mathrm{y}_p$ and z are the final result of interior orientation that can be used in the procedure of bundle adjustment as measurements.

2.2 Exterior Orientation Modeling

Exterior Orientation (EO) parameters, which are the positions of the camera perspective center and bundle pointing angles at a specific time, are provided in SPICE kernels. The EO parameters of each image line can be retrieved by interpolating the spacecraft's trajectory and pointing vectors. Previous researches prove that the change of EO parameters in short trajectories can be well modeled using polynomials (Yoon and Shan 2005). In this research, second-order polynomials are used to model this change

$$\begin{aligned} X^c{}_i &= a_0 + a_1 t + a_2 t^2 & \omega^c{}_i &= d_0 + d_1 t + d_2 t^2 \\ Y^c{}_i &= b_0 + b_1 t + b_2 t^2 & \varphi^c{}_i &= e_0 + e_1 t + e_2 t^2 \\ Z^c{}_i &= c_0 + c_1 t + c_2 t^2 & \kappa^c{}_i &= f_0 + f_1 t + f_2 t^2 \end{aligned} \quad (4)$$

where $X^c{}_i, Y^c{}_i, Z^c{}_i$ are the position of the perspective center of the sensor of the i^{th} point; $\omega_i, \varphi_i, \kappa_i$ are the pointing angles of the i^{th} point; $a_0 \ldots f_2$ are the polynomial coefficients and t is the time-dependent image row index number. Modeled this way, EO parameters can be adjusted by modifying the 36 polynomial coefficients of the stereo pair. The complexity of the adjustment is significantly reduced by this method.

Since all 14 CCDs are fixed to the HiRISE frame, they share the same perspective center and focal plane. Therefore, changes of the EO parameters of all 14 CCDs yield one set of polynomial coefficients. This critical characteristic significantly reduces the complexity of the bundle adjustment on HiRISE stereo images. Images simultaneously generated by multiple CCD arrays can be processed together under a uniform rigorous camera model in the bundle adjustment instead of being processed strip by strip.

To apply the strategy above, one reference CCD strip must be assigned; this strip could be arbitrarily chosen. Then the offsets between other CCD strips and the reference strip are calculated by comparing their EO data line by line. The row index of the

EO polynomials of the reference strip starts from zero. For the other non-reference strips, it starts from the offsets. The initial value of the EO polynomial coefficients can be figured out by least-squares fitting of the line-by-line telemetry EO data.

3. BUNDLE ADJUSTMENT OF HiRISE STEREO IMAGES

This bundle adjustment integrates HiRISE EO parameters and tie points on HiRISE stereo images. EO parameters have been retrieved from the SPICE kernel and stored line by line. A hierarchical-matching algorithm has been developed at the Mapping and GIS Laboratory at The Ohio State University (OSU) for mapping purposes. The tie points are automatically selected from the matched terrain points on stereo images to make sure they are evenly distributed. These tie points will be included in the bundle adjustment as measurements after the interior orientation procedure.

Different types of measurements will form observation equations separately. For image tie points, they are related to the ground coordinates and EO parameters via the collinear equations:

$$x_i + f\frac{a^i_{11}(X_i - X^c_i) + a^i_{12}(Y_i - Y^c_i) + a^i_{13}(Z_i - Z^c_i)}{a^i_{31}(X_i - X^c_i) + a^i_{32}(Y_i - Y^c_i) + a^i_{33}(Z_i - Z^c_i)} = 0$$
$$y_i + f\frac{a^i_{21}(X_i - X^c_i) + a^i_{22}(Y_i - Y^c_i) + a^i_{23}(Z_i - Z^c_i)}{a^i_{31}(X_i - X^c_i) + a^i_{32}(Y_i - Y^c_i) + a^i_{33}(Z_i - Z^c_i)} = 0 \quad (5)$$

where x_i is the along-track coordinate of the detector on the focal plane of the i^{th} point which can be calculated using HiRISE interior orientations; y_i is the corresponding cross-track image coordinate; X_i, Y_i, Z_i are the ground coordinates of the i^{th} point; X^c_i, Y^c_i, Z^c_i are the position of the perspective center of the sensor at the i^{th} point; $a^i_{11} ... a^i_{33}$ are the elements of the rotation matrix formed by the sensor pointing angles, and f is the focal length of the sensor.

The EO parameters in Equation 4 determined through sensor modeling are treated as weighted parameters to form a set of pseudo observation equations, such that

pseudo observation + correction – parameter = 0 (6)

These equations are combined into the bundle adjustment system. The adjustment is based on the least-squares principle minimizing the sum of the weighted square of the residuals of the observations and the pseudo observations. Since Equation 5 is non-linear, linearization should be applied. Therefore the solution must be iterative. The initial values of the EO polynomial coefficients are from the least-squares fitting of telemetry EO data. The initial ground positions of tie points are obtained through an intersection using telemetry EO data.

In this bundle adjustment system, tie points are used as measurements and telemetry EO parameters serve as pseudo measurements; 36 EO polynomial coefficients and ground tie point coordinates are unknowns. One tie point contributes to 4 measurements and 3 unknowns, therefore at least 36 tie points are needed to make the problem solvable.

4. DATA PROCESSING RESULTS AT MER SITES

4.1 Bundle Adjustment without Ground Control

The MRO mapping data used in this study includes HiRISE stereo images and MRO trajectory data including the positions of the camera perspective center and pointing angles. Table 1 summarizes the main properties of the stereo images used in this study.

Site Name	Victoria Crater		Husband Hill	
Stereo	Left	Right	Left	Right
Acquisition Time (M/D/Y)	10/03 /2006	11/14 /2006	12/12 /2006	11/22 /2006
Convergence Angle	9.8 degrees		19.8 degrees	
Image Size	5000 by 4096		5000 by 4096	
No. of Tie Points	136		178	

Table 1. Sites studied in this research

Victoria Crater and Husband Hill, where the twin rovers in the 2003 Mars Exploration Rover (MER) mission are doing their surface exploration, were selected as mapping areas in this study. The planned comparison with ground mapping products and further integration with ground data was the reason those sites were chosen. Also, those two sites represent two typical geological characteristics on the Martian surface. Husband Hill is a hilly area with a lot of topographical variations while Victoria Crater is 800 meters in diameter with a very smooth crater wall and flat sandy surface outside the crater ring. MRO trajectory data is extracted using Spacecraft, Planet, Instrument, C matrix (sensor orientation) and Event (SPICE) library provided by NASA's Navigation Ancillary Information Facility (NAIF). The navigation data is stored as kernels and can be accessed by time (Yoon and Shan, 2005). The acquisition time and number of image lines can be retrieved from each image header. Plugging them into the SPICE kernel will generate the line-by-line telemetry trajectory data needed in this study.

Different from the situation on earth, no absolute ground truth is available on the Martian surface. Therefore, the performance of the bundle adjustment was evaluated in terms of back-projection residuals in image space. The refinement of EO parameters was also analyzed.

Bundle adjustment aims at removing the inconsistencies between HiRISE stereo images by adjusting their EO parameters. The refined EO parameters are compared with those obtained from telemetry data. Figure 2 presents their differences in graphic format. The horizontal axis of Figure 2 is the image row index and the vertical axis is the difference.

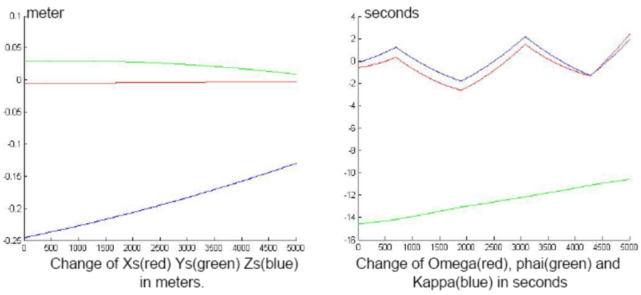

(a) Victoria Crater

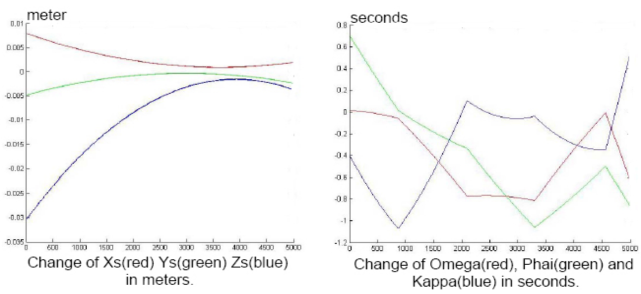

(b) Husband Hill

Figure2. Difference between telemetry and refined EO

Besides the tie points, a comparable number of evenly distributed check points independent from the bundle adjustment were also evenly selected for evaluation. The differences between check point measurements and ground check point back-projection on the image, called back-projection residuals, represent the inconsistencies between HiRISE stereo images. Figure 3 shows the back-projection residuals on the images covering the two sites before and after bundle adjustment; table 2 shows the corresponding statistics.

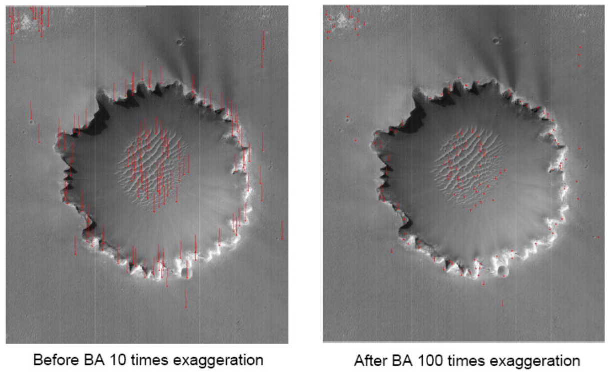

(a) Victoria Crater

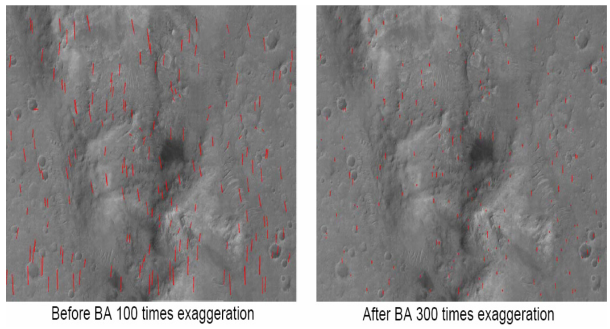

(b) Husband Hill

Figure3. Check point back projection residuals on the images

Site	Victoria Crater		Husband Hill	
Status	Before BA	After BA	Before BA	After BA
Mean(pix)	-26.4	-0.3	-0.5	0.0
Max(pix)	-29.2	-1.4	4.1	0.5
Std(pix)	0.81	0.3	2.0	0.2
No. of Points	135 check points		180 check points	

Table 2. Statistics on back-projection residuals at both sites

Results show that along-track error is more significant than cross-track error before adjustment. A possible explanation is that telemetry EO greatly depends on the accurate time measurement. Any error in time measurement will more greatly affect on the along-track direction in which the satellite is moving. After bundle adjustment, along-track error greatly reduced. This corresponds to the larger correction of φ and Z_S compared to other pointing angles and position elements as is showed in Figure 2. It is noted that Z_S is mostly along track because both sites are in equatorial area. Finally, comparing the two data sets studied, Husband Hill images shows smaller back projection residuals before BA and smaller EO refinement after BA. This indicates that telemetry EO might have been improved during the period between taking the two stereo pairs.

4.2 Bundle Adjustment with Ground Control

To demonstrate the possibility of integrated bundle-adjustment using both orbital and ground rover imagery, points measured from bundle-adjusted Spirit rover images were incorporated into the HiRISE bundle adjustment as control points using Husband Hill data set. During 4 years of rover localization operations at the Mapping and GIS Laboratory at OSU, a 10-kilometer bundle-adjusted traverse of the Spirit rover was generated. An localization accuracy of 0.2 percent of the whole traverse distance was achieved. Three dimensional (3D) ground coordinates of four distinguishable topographic features were measured from the bundle-adjusted rover images and corresponding features were identified on the HiRISE stereo images (Figure 4). Following equations in Wang 1990, the 3D coordinates of the four points were transformed from the Local Tangent Plane Coordinate System to the Mars Body-fixed Coordinate System and then used as control points in the bundle adjustment. Just as with the tie points, image coordinates of the control points were related to the ground control points and EO parameters using Equation 4. But unlike tie points, the control point ground positions do not vary during the iteration process.

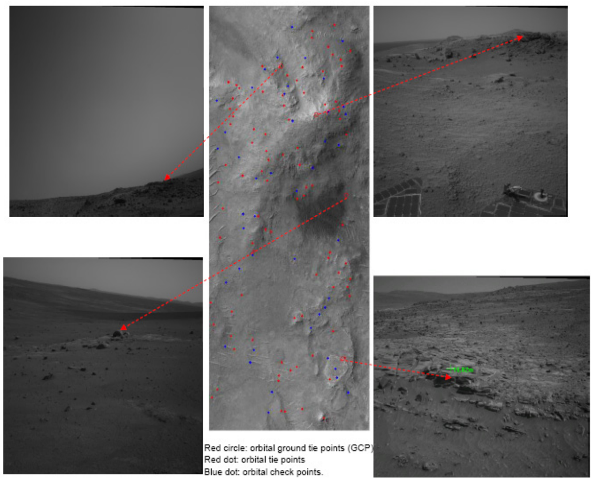

Figure 4. Point distribution and correspondence between orbital and ground imagery (Red Circle: GCP; Red Dot: tie point; Blue Dot: check point)

With rover imagery incorporated, the inconsistencies between orbital and ground imagery becomes another criterion of performance for the bundle adjustment. First, the 3D ground coordinates of a topographic feature are measured from rover stereo images. Afterwards, the ground coordinates of the same feature are intersected using HiRISE stereo images based on both telemetry and bundle-adjusted EO parameters. In order to remove the systematic shift between orbital and ground imagery, a 3D translation is conducted before BA so that the positions of the first point from both orbital and ground imageries are identical. The comparison of the positions derived from orbital imagery and rover imagery are showed in Table 3.

	Before BA			After BA		
	dX(m)	dY(m)	dZ(m)	dX(m)	dY(m)	dZ(m)
Point1	0	0	0	-0.04	-0.32	-0.06
Point2	21.6	-17.1	-2.74	0.67	0.08	0.18
Point3	49.2	-32.3	-10.4	3.70	1.85	-0.06
Point4	61.0	-7.62	-51.6	2.07	-1.00	1.33

Table 3. The difference between orbital and ground based ground control points measurement before and after HiRISE BA with control from Spirit rover imagery.

The results show that the inconsistencies between orbital and ground imageries can be reduced from dozens of meters to several meters or even sub-meter level by very simple integration without considering error accumulation in the rover traverse. Therefore, topographical accuracy could be further improved by integrating ground measurement into HiRISE bundle adjustment.

5. INVESTIGATION OF JITTER

Small motions of spacecraft around its nominal pointing, called jitter, will distort the images. This problem was identified for Mars Orbiter Camera (MOC) images, but it is more severe for HiIRISE because of HiRISE's higher resolution (R. Kirk, 2007). High-frequency jitter can be filtered out by subtracting the best fitting polynomial from the original telemetry HiRISE pointing angle data. An 80,000 line image in Gusev Crater was used in this study. Figure 5 shows the extracted jitter on ω, φ, κ, with the horizontal axis as image row index and vertical axis as jitter magnitude in arc-seconds. An analysis to the extracted residuals in spectral domain does not show any frequency significance. Therefore, it could be very difficult to incorporate this "jitter" into a mathematical model.

Jitter, as is caused by unpredictable action forces on the camera, cannot be modeled by polynomials and therefore, it can not be solved by bundle adjustment. Thus, the topographic effect of orbital jitter must be evaluated for topographic capability analysis of HiRISE camera. For evaluation, a single CCD pixel was projected onto the Martian surface using telemetry EO data under the assumption that Mars is a sphere with its radius derived from the nearest MOLA point. The projected footprint was compared with another projected footprint using EO parameters from second-order polynomials under the same spherical assumption. A maximum difference of 2 meters, corresponding to 7 pixels, was detected from the comparison in this 20-kilometer track on the Martian surface. However, for a small mapping area (for example, one square kilometer), the effect is smaller than 0.1 meter on the ground. This corresponds to only one third of a pixel on the image which is insignificant. However, further investigation on jitter will be performed so that its effects can be removed or reduced when mapping large areas.

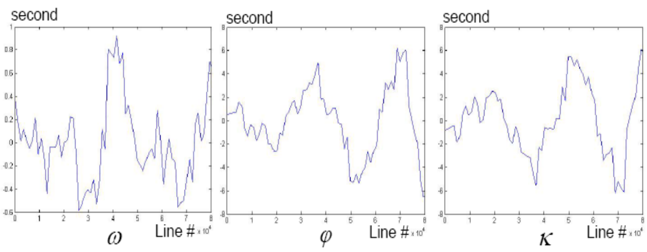

Figure 5. Residuals after subtracting best fitting polynomial from original telemetry EO data

6. CONCLUSIONS

The rigorous geometric model for HiRISE is developed in this paper incorporating the sensor calibration data provided by USGS. Mosaic of multiple image strips taken by HiRISE could be processed simultaneously under this rigorous model instead of strip by strip. Based on this model, a bundle adjustment is developed and implemented on HiRISE stereo pairs covering both Husband Hill and Victoria Crater. Along with precise image tie point measurements, trajectory data are also incorporated as pseudo measurements to enhance the geometry. HiRISE EO parameters are adjusted based on these measurements. Results from both study sites indicate that bundle adjustment successfully removes the inconsistencies between two images in a stereo pair. Four points measured from both HiRISE stereo images and geo-registered Spirit rover images are used as ground control points linking the orbital and ground geometry. Incoporating these control points, another bundle adjustment is implemented on Husband Hill stereo pair. The significantly reduced residuals on the ground features between orbital intersection and measurements from rover images show the potential of further orbital-ground integration. The effect of orbital jitter, which is small motions of spacecraft around its nominal pointing, is evaluated in this paper. This study suggests that the topographic effect of jitter is insignificant when mapping small areas; however, further investigation on jitter needs to be performed so that its effect can be removed or reduced when mapping large areas.

ACKNOWLEDGEMENT

This work is sponsored by the National Aeronautics and Space Administration (NASA).

REFERENCES

McEwen. A, E.M. Eliason, J.W. Bergstrom, N.T. Bridges, C.J. Hansen, W.A. Delamere, J.A. Grant, V.C. Gulick, K.E. Herkenhoff, L. Keszthelyi, R.L. Kirk, M.T. Mellon, S.W. Squyres, N. Thomas, and C.M. Weitz, Mars Reconnaissance Orbiter's High Resolution Imaging Science Experiment (HiRISE). Journal of Geophysical Research, Vol. 112, E05S02

Yoon J-S and Shan J. Combined Adjustment of MOC Stereo Imagery and MOLA Altimetry Data Photogrammetric Engineering & Remote Sensing Vol. 71, No. 10, October 2005, pp. 1179–1186

Kirk R.L., E. H. Kraus, M.R. Rosiek1, D. Cook, J. Anderson, K. Becker, B.A. Archinal, L. Keszthelyi, R. King, A.S. McEwen and the HiRISE Team. Ultrahigh Resolution Topographic Mapping of Mars with HiRISE Stereo Images: Methods and First Results. Seventh International Conference on Mars July 9-13, 2007 Pasadena, CA

Shan J., J-S Yoon, D.S. Lee, R.L. Kirk, G.A. Neumann, and C.H. Acton. Photogrammetric analysis of the Mars Global Surveyor mapping data, Photogrammetric Engineering & Remote Sensing, Vol.71, pp. 97–108

Wang, Z.Z., 1990. Principles of Photogrammetry (with Remote Sensing), Press of Wuhan Technical University of Surveying and Mapping, Publishing House of Surveying and Mapping, Beijing, 575 pages.